Simulations of a DIII-D Plasma Disruption with the NIMROD Code

S.E. Kruger 1), D.D. Schnack 2),

1) Tech-X Corporation, Boulder, Colorado, USA
2) SAIC, San Diego, California, USA

e-mail contact of main author: kruger@txcorp.com

Abstract. To investigate the dynamics of the disruption of DIII-D discharge number 87009, two types of initial-value simulations with the NIMROD code were performed to investigate different characteristics. In the first set of simulations, a conducting wall was placed on the last close flux surface, and an equilibrium that was close to the ideal-MHD marginal stability point was created. A heating source was added to the pressure equation to drive the plasma equilibrium through an ideal-MHD instability point. Excellent agreement with analytic theory was obtained. To investigate how the stored energy is deposited on the wall, free-boundary simulations were performed with an ideal-MHD unstable equilibria. The unstable modes grow until the magnetic islands overlap and the magnetic field is stochastic over a large part of the plasma domain. The rapid stochastization of the field allows the plasma to lose two thirds of its internal energy in approximately 200 microseconds in qualitative agreement with the experiment. The deposition of thermal energy on the wall is localized poloidally and toroidally on the wall due to helically-localized temperature gradients and the rapid parallel heat conduction which carries this heat flux to the wall.

1 Introduction

The experimental phenomenology of the disruption in DIII-D discharge 87009 has attracted a great deal of theoretical interest [2-5]. A combination of analytic theory [2] and linear ideal MHD code analysis [3] has been successful in predicting both the time scale of the disruption [2] and the spatial structure [3] of the mode. The success of the model and the indication that the phenomenology can be described with strictly a magnetohydrodynamic model makes this an attractive case to study with the NIMROD [6] nonlinear initial-value code. Unlike the simple analytic/linear numerical MHD model, an initial-value code allows for detailed studies of the mechanism leading to the loss of plasma confinement and the resultant heat deposition on the plasma wall.

This paper presents two different NIMROD simulations. In the first, the time-dependent behavior is modeled using a fixed boundary equilibria. The emphasis of this simulation is to numerically validate the analytic model of Reference [1]. In the second simulation, the NIMROD simulation starts from a free-boundary equilibrium that is above the ideal MHD threshold. The emphasis in this simulation is to model how the heat flux gets deposited on the wall. In the final section, conclusions are drawn and further work is discussed.

2 Fixed-boundary simulations

Typical initial-value MHD simulations of tokamak plasmas have been performed with the conducting boundary on the last closed flux surface. Fixed-boundary simulations have two advantages: 1) they avoid the numerical difficulties associated with allowing the large-gradients near the boundary to move, and 2) it is much easier to create equilibria that have some desired property, such as proximity to marginal stability. To investigate the time-dependent behavior of a plasma disrupting as it is heated through an ideal-MHD instability, a series of fixed-boundary simulations was performed with the NIMROD code.

Instabilities observed in plasmas are typically classified by the time scales associated with their growth (with the ideal modes growing on the Alfvenic time scale, and the other modes having a time scale that is a hybrid of the Alfvenic and resistive time scales) and by calculating the stability of the reconstructed equilibrium with linear eigenvalue codes.[2] However, this traditional type of analysis neglects how the plasma reached an unstable equilibrium. Recently, an analytic theory [1] has been put forth to describe the growth of an instability being driven through the marginal stability point. Assuming that the free energy of the mode is proportional to β, then

$$\omega^2 = \frac{\delta W}{\delta K} \sim -\hat{\gamma}_{MHD}^2 \left(\frac{\beta}{\beta_{crit}} - 1 \right). \tag{1}$$

Assuming a slow heating rate so that the heating may be approximated as a linear increase in β with a heating rate γ_h near the marginal point, $\beta(t) = \beta_{crit}(1 + \gamma_h t)$, one obtains a growth rate that depends on the heating rate with the resultant mode growing faster than exponential:

$$\xi = \xi_0 \exp\left[(t/\tau)^{3/2} \right]. \tag{2}$$

The time constant of the mode is a hybrid of the variation of the growth rate with beta and the heating time scale:

$$\tau \equiv \frac{(3/2)^{2/3}}{(\hat{\gamma}_{MHD})^{2/3} \gamma_h^{1/3}}. \tag{3}$$

As the limit of either $\hat{\gamma}_{MHD}$ or γ_h goes to zero, the mode does not grow because it is exactly at the marginal point.

This heuristic analytic theory was successfully used to explain many of the features of DIII-D discharge 87009 which disrupted during neutral-beam heating [1], including the time-scale that was deemed to be too slow for an ideal mode. An interesting part of this derivation is the use of linear theory to model the instability which is observed in the nonlinear regime. To further test this theory and gain additional insight into the nonlinear behavior, discharge 87009 was modeled using the nonlinear resistive MHD equations with anisotropic heat conduction with an equilibrium with similar pressure and safety factor profiles as the actual discharge at 1681.7 msec.

Before running a self-consistent nonlinear simulation with heating, it is necessary to begin the simulation near the ideal marginal stability point. Because having a conducting

wall placed on the last closed flux is stabilizing, the plasma pressure was raised to the ideal marginal stability point by self-similarly increasing the plasma pressure profile. To determine the critical beta with sufficient accuracy, the equilibrium was varied from $\beta_N = 4.0$ to $\beta_N = 5.0$ in increments of $\Delta\beta_N = 0.05$. The ideal linear stability of the equilibria was tested with DCON [3] to determine plasma stability to ideal modes using a generalized version of Newcomb's criterion [4]. Because linear calculations with NIMROD take much longer than DCON to determine ideal stability, using DCON on a large number of equilibria is generally preferred. The ideal marginal stability point was found by DCON to be $\beta_N = 4.45$. Linear NIMROD simulations found resistive interchange modes at $\beta_N = 4.0$, and the extremely robust growth rates expected of ideal instabilities at $\beta_N = 5.0$ and $\beta_N = 6.0$. Because the growth of the mode at $\beta_N = 4.45$ is very slow, we consider it to be *computationally stable* (with regards to ideal instabilities) and we chose $\beta_N = 4.70$ as the starting point for our calculations.

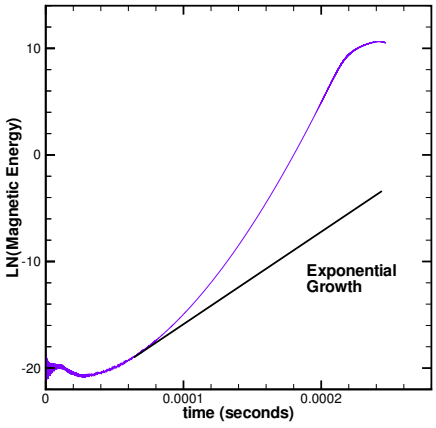

FIG. 1: The $n = 1$ perturbation grows faster than exponential as predicted by analytic theory.

To model the heating of the plasma, a heating source is added to the pressure equation: $Q = \gamma_h p_{eq}$. The NIMROD simulations were run with Lundquist number $S = 10^6$, Prandtl number (ratio of normalized resistivity to kinematic viscosity) $Pr = 200$ with heating rates of $\gamma_h = 10^{-3}\ s^{-1}$ and $\gamma_h = 10^{-2}\ s^{-1}$. Because our heating rate is slow compared to the growth of the mode, but still much faster than the resistive decay time ($\hat{\gamma}_{MHD} \gg \gamma_h \gg 1/\tau_R$), the assumptions of the analytic theory [1] are satisfied. A finite-element grid in the poloidal plane with 128 radial vertexes and 64 poloidal vertexes was used with cubic polynomial Lagrangian elements [5]. The toroidal direction is discretized using the pseudo-spectral method using the $n = 0$ and $n = 1$ modes. Only the first two modes are kept because the higher n modes are substantially destabilized due the necessary increase in beta to make the $n = 1$ mode unstable in the presence of a conducting wall on the boundary. Our results are only qualitatively correct in the fully nonlinear regime, but the goal is to explore the behavior in the experimentally-relevant quasi-linear regime and compare the results to the analytic theory. Note that throughout the simulations, NIMROD's finite-element grid

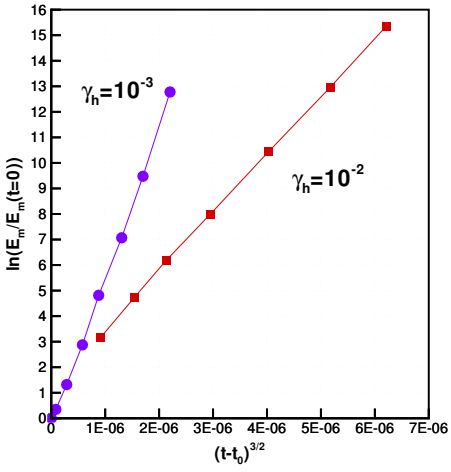

FIG. 2: Plotting the log of the magnetic energy, E_m, versus the the normalized time raised to $3/2$ power shows excellent agreement with the analytically-predicted scaling behavior as evidenced by the straight lines.

is aligned to the equilibrium magnetic field and does not move although the flux surfaces shift outward as the plasma heats.

The results of the NIMROD simulation with $\gamma_h = 10^{-3}\ s^{-1}$ are shown in Figure 1. As predicted by the analytic theory, the growth of the mode is faster than exponential. This faster-than-exponential growth satisfies Eq. (2) well into the nonlinear regime. as represented by the straight lines in the fitting shown in Figure 2. Using the slopes of the lines in Figure 2 to determine the time constant for each heating rate gives a fit to the time constant of

$$\tau \sim \hat{\gamma}_{MHD}^{-0.72} \gamma_h^{-0.28} \tag{4}$$

which agrees well with the analytic prediction given by Eq. (3).

3 Free-boundary simulations

To minimize the interactions of the hot plasma with the cold wall, modern tokamaks divide the plasma into two distinct regions: a core region where field lines close upon themselves and confine the plasma ($T_e \sim 10$ keV in DIII-D) , and a "halo" region where the field lines intersect the wall and the plasma remains cold ($T_e \sim 10$ eV in DIII-D). The separatrix which divides the two regions is only clearly defined in a two-dimensional magnetic field – in three dimensions a stochastic region exists in general that blurs the separation. NIMROD's use of high-order elements [5] allows the accurate modeling of the heat flux required to resolve the distinction between the halo region and core region as the plasma evolves nonlinearly.

The simulation was initiated from an equilibrium based on the best equilibrium reconstruction at 1675 ms. Because starting below the critical ideal MHD threshold adds com-

putational cost to an already expensive calculation, the equilibrium pressure was raised self-consistently by 8.7% above the best equilibrium reconstruction to place the plasma beta above the ideal MHD threshold.

The simulations presented were run with a temperature dependent resistivity normalized such that the Lundquist number in the core plasma was $S = 10^5$. A ratio of $\kappa_\parallel/\kappa_\perp = 10^8$ was held constant throughout the computational domain. The boundary conditions are applied at the vacuum vessel (modeled as a perfectly conducting wall), and not the first material wall. The normal component of the magnetic field is held constant at the conducting surface. The boundary conditions are also applied at the vacuum vessel instead of the more physical limiter surface for the density, velocity, and temperature.

In Figure 3, the global parameters of internal energy and plasma current from the NIMROD simulation are shown. The plasma energy decreases by two-thirds in approximately 200 microseconds in qualitative agreement with the experiment. Because constant voltage boundary conditions are used in this simulation, the plasma current changes as reconnection processes occur inside the plasma and the internal inductance changes.

As the temperature evolves during the simulation, the first notable macroscopic feature is the appearance of a $2/1$ island, as seen in Figure 4(a). Two magnetic field lines started near the same point are shown. They are colored according to the temperature along their path, and the brightness of the nodes indicates the distance along the fieldline to aid in the visualization. At this time step, the temperature has equilibrated sufficiently that the island can be seen in the temperature isosurface, although significant variations of the temperature along the magnetic field line are beginning to occur. As the plasma evolves, secondary islands are generated and overlap causing stochasticization over most of the domain.

At time of maximum heat flux, Figure 5(a), the heat flux is localized toroidal on both the top and bottom divertors, 180 degrees apart. There is also a significant poloidal structure to the heat flux. Exploring the topology of the magnetic field in more detail, in the isosurfaces of Figure 5(b), we see that the locations of maximum heat flux are connected by a magnetic field line. Because the heat transport along magnetic field lines is much more rapid than heat transport across field lines, any heat flux that reaches the open field lines is able to quickly equilibrate and reach the plasma boundary. The localization of seen on the divertor region is therefore a consequence of localization of heat flux within the core plasma. The localization of heat flux within the core plasma results from the initial perturbation, which distorts and compresses the temperature surfaces and raises the heat flux.

4 Discussion and Conclusions

Despite the heuristic nature of the analytic derivation of mode growth being driven through an ideal marginal instability point, the NIMROD simulations show that the analytic scaling given by Eq. (2) gives an excellent description of the mode growth even into the nonlinear regime. For ideal modes, where the mode amplitudes can grow quite large with a change in magnetic topology, the fundamental assumptions of the analytic theory holds into the nonlinear regime. The simulations emphasize the importance of simulating not only the

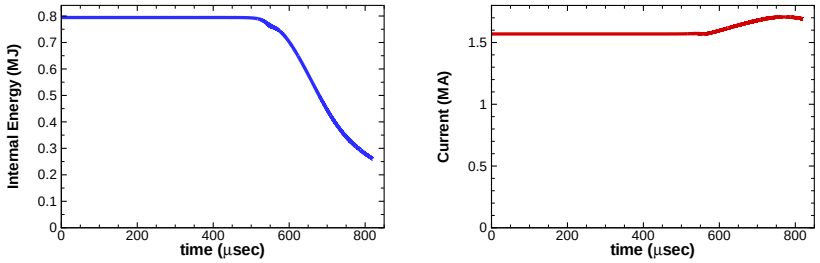

FIG. 3: The plasma loses two-thirds of its internal energy in 200 μs, in qualitative agreement with experiment. Because constant voltage boundary conditions are used, the current rises during the reconnection events in the plasma.

instability, but the mechanism by which the plasma has evolved to that state. Unfortunately, simulations near the marginality point are the most difficult to simulate due to the slowness of the mode growth.

The free boundary simulations which explored the realistic DIII-D geometry and heat flux deposition shows many of the qualitative features of plasma disruptions. The macroscopic loss of energy confinement time of 200 microseconds is in qualitative agreement with experiment. The localization of the heat flux, both toroidally and poloidally is observed during disruptions in detail. The heat flux localization arises because of the magnetic topology resulting from the internal reconnection events. Rapid temperature equilibration carries the localized heat loads to the divertor walls. Qualitative agreement with the experiment did not require the use of complicated plasma-wall interactions. This is primarily because the plasma stayed relatively well-confined within the original last-closed flux surface, and the time-scale of the mode growth is rapid compared to the time-scale of impurity penetration. For disruptions where mode growth occurs on a slower time scale, modeling of impurities in the NIMROD code would be necessary.

Future work will include more accurate modeling of the heat flux, including temperature-dependent Braginskii coefficients, use of Landau-fluid closures, [6,7] a kinetic calculation of heat flux, [8,9] resistivity value to overcome the main weaknesses of the current set of numerical experiments: the use of a Braginskii heat flux model with constant coefficients and the use of artificially high resistivity. Future simulations will also try to drive the free-boundary simulations through the stability point in the same way the fixed-boundary equilibria were driven. By more accurately modeling the time-dependence and physical parameters, quantitative comparisons can be made. This will allow us to explore the role of the external magnetic configuration in the role of the heat deposition.

5 Acknowledgements

This work was strongly motivated by the work of and discussions with Dr. J.D. Callen. Drs. M.-S. Chu, and A. Turnbull provided the equilibria used in this study, and many useful insights based upon their previous work. Dr. A. Tarditi participated in several discussions.

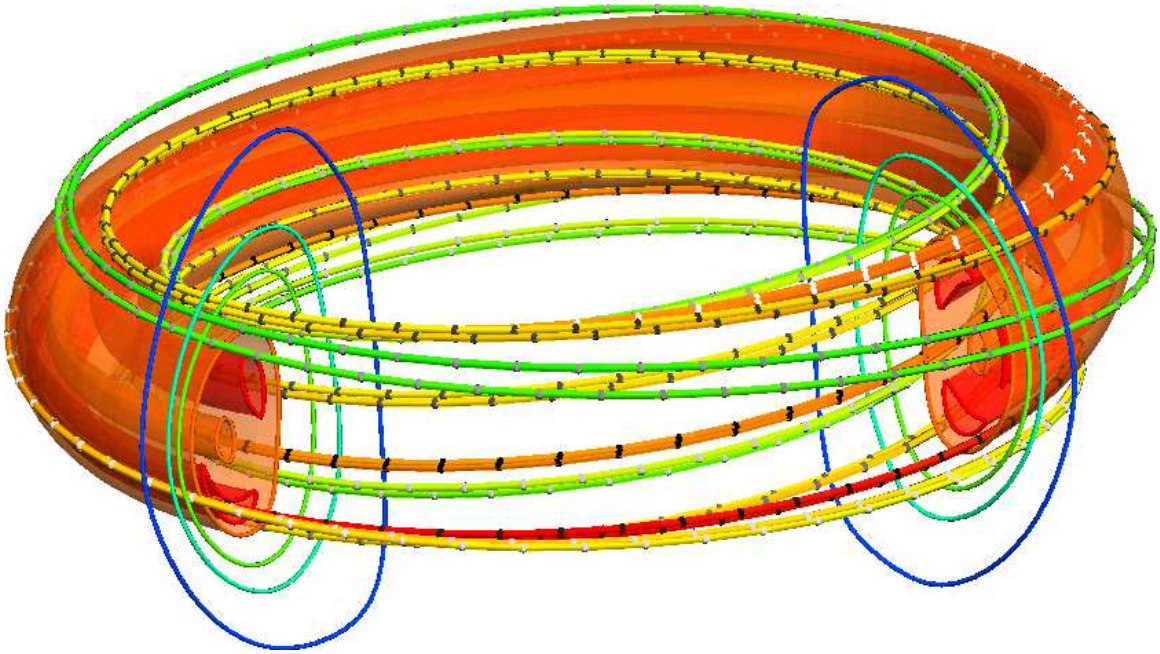

FIG. 4: The first macroscopic feature in the temperature isosurfaces, is the $2/1$ island.

Dr. C.R. Sovinec provided many useful suggestions which made these simulations numerically possible. This work was performed under U. S. DOE contract DE-FE03-02ER5466.

References

[1] CALLEN, J.D., *et.al.*, Phys. Plasmas, **6**, 2963 (1999).
[2] STRAIT, E.J. Phys. Plasmas, **1**, 1415 (1994).
[3] A.H. GLASSER, *private communication*
[4] NEWCOMB, W.A., Annals of Physics, **10**, 362 (1960).
[5] SOVINEC, C.R., *et.al.*, J. Comp. Phys., **195**, 355 (2004).
[6] HAMMETT, G.W. AND Perkins, F.W., Phys. Rev. Lett., **64**, 3019 (1990).
[7] SNYDER, P.B., *et.al.*, Phys. Plasmas, **4**, 3974 (1997).
[8] HELD, E.D. *et.al*, Phys. Plasmas, **8**, 1171 (2001).
[9] HELD, E.D. *et.al*, Phys. Plasmas, **11**, 1171 (2004).

(a)

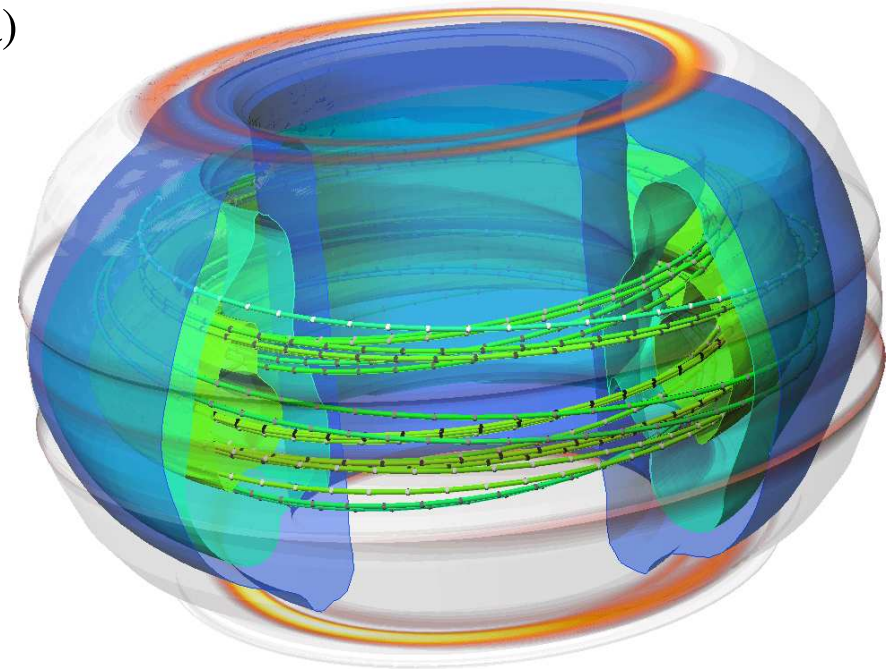

(b)

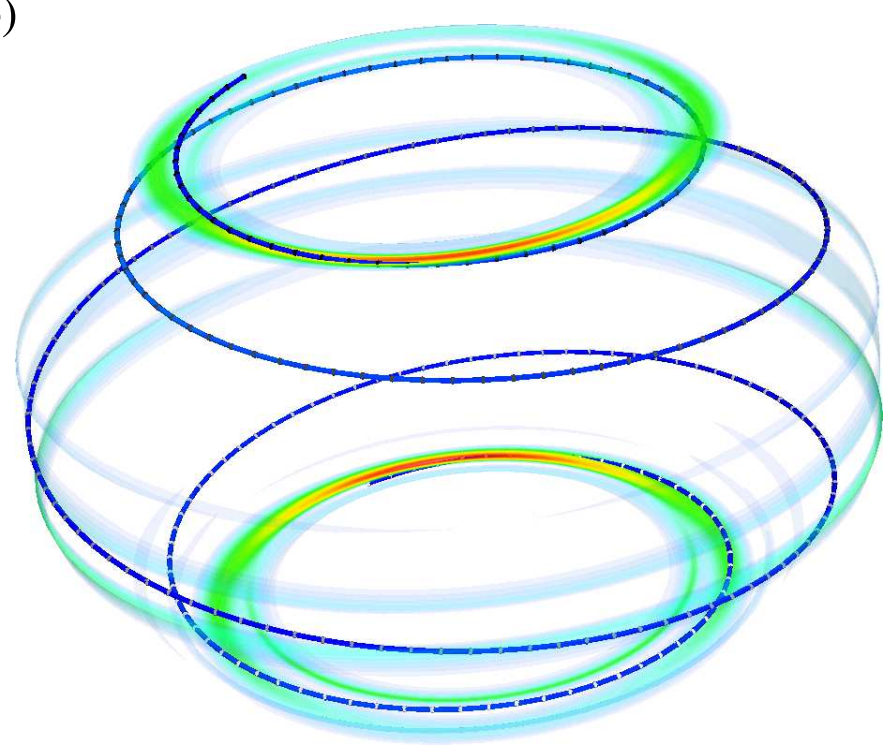

FIG. 5: